Plasticity of motor corticobulbar projections following different lesion types affecting the central nervous system in adult macaque monkeys

Rouiller EM[1], Fregosi M[1], Contestabile A[1], Badoud S[1], Borgognon S[1], Cottet J[1], Brunet JF[2], Bloch J[2], Schwab ME[3]

1 Departement of Neuroscience, Univ. of Fribourg; 2: Neurosurgery Department, Univ. of Lausanne; 3: Brain Research Institute, Univ. of Zürich; Switzerland.

Poster D072 - Abstract F18-0147

INTRODUCTION

The corticobulbar projection, together with the corticospinal tract (CST), act in parallel with projections from the brainstem (such as the reticulospinal tract) to ensure direct or indirect control of movement on motoneurons in the spinal cord.
In monkeys little is known about the projections coming from the motor cortex on the brainstem as well as on their influence. Previous studies suggested a role of the reticulospinal tract in the control of reaching movement and in the recovery after a lesion of the CST, spinal cord or cerebral cortex.
The aim of the present study was to anatomically analyze and compare the corticobulbar projections on the ponto-medullary reticular formation (**PMRF**) of the brainstem, possibly influencing the reticulospinal neurons. Corticobulbar projections were previously reported in intact monkeys, originating from the premotor cortex (PM), the supplementary motor area (SMA) and the primary motor cortex (M1): see Fregosi et al., 2017 (EJN). In the present study, we report on the changes of the motor corticobulbar projections onto PMRF after injury of either the primary motor cortex (**MCI**), or spinal cord injury (**SCI**), or Parkinson's Disease like lesions of the nigro-striatal dopaminergic system (**PD**).

METHODS

The tracer biotinylated dextran amine (BDA) was injected unilaterally in either PM or M1 of thirteen lesioned adult macaque monkeys (*Macaca fascicularis*). The corticobulbar projections anterogradelly labeled with BDA were then analyzed in 12 consecutive histological sections (50 µm thick), 250 micrometers apart. Stem axons and terminals, including boutons *en passant*, were then plotted using the software Neurolucida.
An adjacent series of 12 sections was stained with Cresyl Violet, revealing Nissl bodies, was used to delineate the brainstem nuclei.
The Neurolucida software is connected to a light microscope (Olympus Bx40). We used the magnification 40x to trace the contours of the sections and the Pyramidal tract, the 100x to trace the axons and finally the 200x to plot the boutons *en passant* and *terminaux*. For the series of sections stained for Nissl we used 12.5x magnification to delineate the nuclei.
Both series of sections (BDA and Nissl) were overlapped in order to match the zones of BDA staining and the nuclei delineated with Nissl staining.

The effects of three types of lesion were studied:
1) **Motor cortex injury (MCI)**: Neurotoxic (ibotenic acid) lesion of the hand representation in the primary motor cortex (M1), as previously reported (Hamadjida et al., 2012; Wyss et al., 2013).
2) **Spinal cord injury (SCI)**: Hemisection of the cervical cord at C7 level, as previously reported (Freund et al., 2006, 2007, 2009).
3) **Parkinson's Disease like lesions of the nigro-striatal dopaminergic system (PD)**: Repeated low-dose i.m. infusions of MPTP, as previously reported (Mounayar et al., 2007; Borgognon et al., 2017).

Statistics to compare the numbers of axonal boutons between the two sides of the PMRF were derived from the paired t-test /Wilcoxon tests, represented with asterisks: * $p \leq 0.05$; ** $p \leq 0.01$, *** $p \leq 0.001$.

Abbreviations

6N	Abducens nucleus	ml	Medial leminiscus (sometimes including the Trapezial body)
7N	Facial nucleus	Mo5	Trigeminal motor nucleus
5n	Trigeminal nerve	Pn	Pontine nuclei
7n	Facial nerve	PnC	Pontine reticular nucleus caudalis
8n	Vestibulocochlear nerve	PnO	Pontine reticular nucleus oralis
9n	Glossopharyngeal nerve	Pr	Prepositus nucleus
12N	Hypoglossal nucleus	Pr5	Principal sensory trigeminal nucleus
CN	Cochlear nucleus	Py	Pyramidal tract
Cu	Cuneate nucleus	Raphe	Raphe nuclei
Ecu	External cuneate nucleus	RtTg	Reticulo tegmental nucleus of Pons
Gi	Gigantocellular reticular nucleus	Sol	Solitary nucleus
IO	Inferior olive	SOC	Superior olivary complex
LRt	Intermediate reticular nucleus		

RESULTS

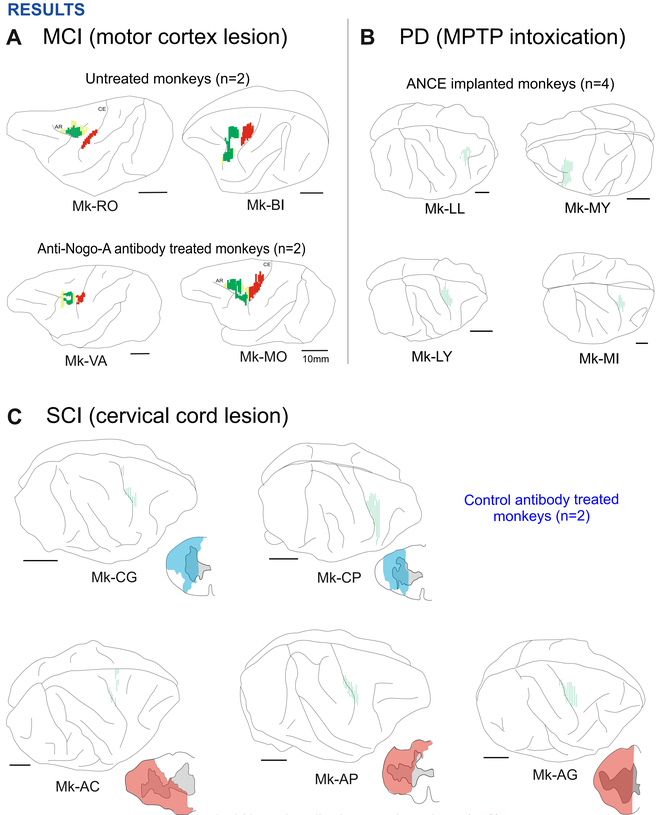

Figure 1

A: On lateral view of the left hemisphere, reconstruction of the BDA injection site in PM (green) and of the M1 lesion (red) for the MCI monkeys (data derived from Hamadjida et al., 2012). For these PM injections, in addition to a dense core region (dark green), an additional halo part was visible where a less dense BDA spread was present. **B**: Lateral view of the hemisphere in PD animals with BDA injection sites (green) in PM (top two monkeys) or in M1 (bottom two monkeys). **C**: Lateral view of the right hemisphere in SCI monkeys with BDA injection sites (green) in M1. Next to each hemisphere, an inset illustrates the cervical cord lesion (blue or red area) in the same monkey, as seen on a frontal section of the cervical cord (derived from Freund et al., 2007; Beaud et al., 2008, 2012). In each panel (A, B, C), the treatment applied to each animal is indicated.

Treatments

Two types of treatments to enhance functional recovery post-lesion were tested:

1) **Anti-Nogo-A antibody treatment**: neutralization of the neurite growth inhibitor Nogo-A, applied to the MCI and SCI groups (see Freund et al., 2006, 2007, 2009; Hamadjida et al., 2012; Wyss et al., 2013).

2) **Autologous neural cell ecosystems (ANCE)**: transplantation of adult neural progenitor cells derived from a healthy part of the cerebral cortex (see Brunet et al., 2005, 2009; Kaeser et al., 2010, 2011; Borgognon et al., 2017). The efficacy of the ANCE treatment in MPTP monkeys in comparison to controls was demontrated earlier (see Bloch et al., 2014).

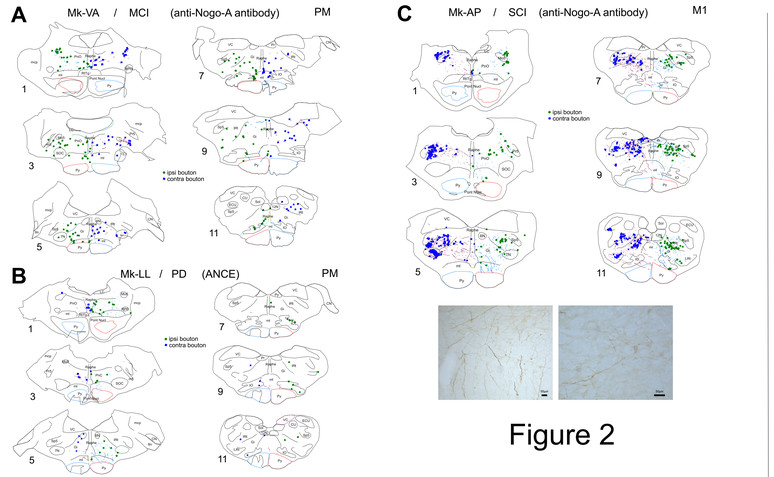

Figure 2

Typical distribution of corticobulbar axonal boutons in PMRF in 6 representative histological sections taken from an MCI monkey (panel A), from a PD monkey (panel B) and from an SCI monkey (panel C). Boutons in the ipsilateral PMRF are depicted in green whereas those in the contralateral PMRF are depicted in blue. In addition, BDA-labelled stem axons are shown in blue on the ipsilateral side and in purple contralaterally. For each monkey, the applied treatment is indicated in parentheses. On each section, the pyramid (Py), when outlined in red, corresponds to the ipsilateral side, with respect to the hemisphere injectedwith BDA (see Fig. 1). See list of abbreviations.

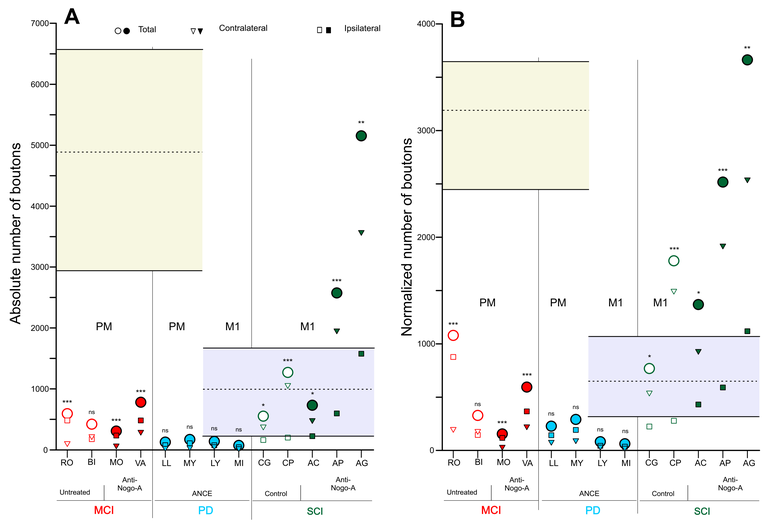

Figure 3

Scatter plots of the numbers of corticobulbar boutons observed in the different groups of monkeys subjected to motor cortex lesion (MCI), spinal cord injury (SCI) or MPTP intoxication (PD). For comparison, the data in intact monkeys (Fregosi et al., 2017) are represented by the range (yellow or light blue area) and the mean value (dashed horizontal line). The yellow area is for data in intact monkeys as a result of BDA injections in PM, whereas the blue area is for data in intact monkeys as a result of BDA injection in M1. In the monkeys subjected to MCI, SCI or PD, the BDA injection site (PM or M1) is indicated below the graph. Panel A is for the absolute numbers of corticobulbar boutons, whereas the panel B is for normalized numbers of corticobulbar boutons. Different symbols display either the total or individual numbers of boutons for the ipsilateral or contralateral PMRF (see legend on top of each panel). The presence/absence of treatment is indicated by filled or open symbols: filled symbols for anti-Nogo-A antibody in MCI or SCI monkeys as well as ANCE treatment in PD monkeys, and open symbols for untreated MCI monkeys or control antibody treated SCI monkeys, respectively. Asterisks above the circle symbols indicate that the numbers of axonal boutons in PMRF were significantly different between the ipsilateral and contralateral sides of PMRF: * is for $p<0.05$, ** is for $p<0.01$, *** is for $p<0.001$, ns is for non-statistically significant difference between the 2 PMRF sides.Normalization (panel B) was performed with reference to the number of BDA-labelled corticospinal (CS) axons above pyramidal decussation level.

Sponsors: Swiss National Science Foundation NCCR neuro and grants 310000-110005, 310003A-132465, 31003A-149643 to EMR.

Brief summary of the corticobulbar projection in intact monkeys

The present study aims at assessing possible changes of the corticobulbar projection in adult monkeys following lesion, such as MCI, SCI or MPTP. This requires a comparison with the corticobulbar projection in intact monkeys, as reported recently (Fregosi et al., 2017). The normal corticobulbar projection to the Ponto-Medullary Reticular Formation (PMRF) is briefly summarized here. First, the corticobulbar projection was found to be clearly denser when originating from PM or the supplementary motor area (SMA) than from M1. This is clearly illustrated in Figure 3 with the comparison of corticobulbar boutons in PMRF originating from PM versus M1 (yellow versus blue areas, respectively). Second, irrespective of the origin, the corticobulbar projection was bilateral although with a predominance on the ipsilateral PMRF when originating from PM or SMA and on the contralateral PMRF when coming from M1. Third, in PMRF, the main nuclei targeted by the corticobulbar projection were the pontine reticular nucleus pars caudalis and oralis (PnC and PnO), the gigantocellular reticular nucleus (Gi), as well as the lateral and intermediate reticular nuclei (LRt and IRt).

Summary of the present study

Functional recovery from central nervous system injury is likely to be partly due to a rearrangement of neural circuits. In this context, the corticobulbar (corticoreticular) motor projections onto different nuclei of the Ponto-Medullary Reticular Formation (PMRF) were investigated in thirteen adult macaque monkeys after either, primary motor cortex injury (MCI) in the hand area, or spinal cord injury (SCI) or Parkinson's Disease-like lesions of the nigro-striatal dopaminergic system (PD). A subgroup of animals in both MCI and SCI groups was treated with neurite growth promoting anti-Nogo-A antibodies, whereas all PD animals were treated with autologous neural cell ecosystems (ANCE). The anterograde tracer BDA was injected either in the premotor cortex (PM) or in the primary motor cortex (M1) to label and quantify corticobulbar axonal boutons terminaux and en passant in PMRF. As compared to intact animals, after MCI the density of corticobulbar projections from PM was strongly reduced but maintained their laterality dominance (ipsilateral), both in the presence or absence of anti-Nogo-A antibody treatment. In contrast, the density of corticobulbar projections from M1 was increased following opposite hemi-section of the cervical cord (at C7 level) and anti-Nogo-A antibody treatment, with maintenance of contralateral laterality bias. In PD monkeys, the density of corticobulbar projections from PM was strongly reduced, as well as that from M1, but to a lesser extent. In conclusion, the densities of corticobulbar projections from PM or M1 were affected in a variable manner, depending on the type of lesion/pathology and the treatment aimed to enhance functional recovery.

CONCLUSION

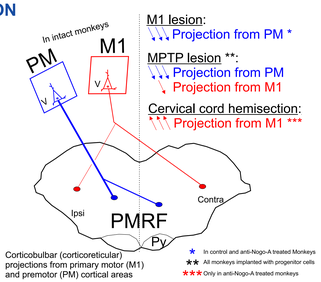

In intact adult macaques, the corticobulbar projections are denser when originating from PM than from M1. After unilateral lesion of M1, the projection from the ipsilesional PM was strongly reduced, both in presence or absence of anti-Nogo-A antibody treatment. After MPTP lesion (and following cell therapy), the projections from both PM and M1 also decreased. In contrast, after cervical cord hemi-section, the projection from M1 increased, but only in presence of anti-Nogo-A antibody treatment.